Fully quantitative description of hybrid TiO2 nanoparticles by means of solid state P-31 NMR

TASSI, Marco; REEKMANS, Gunter; CARLEER, Robert & ADRIAENSENS, Peter
(2016) Fully quantitative description of hybrid TiO2 nanoparticles by means of solid state P-31 NMR. In: SOLID STATE NUCLEAR MAGNETIC RESONANCE, 78, p. 50-55.

DOI: 10.1016/j.ssnmr.2016.07.001
Handle: http://hdl.handle.net/1942/22696

Fully quantitative description of hybrid TiO_2 nanoparticles by means of solid state ^{31}P NMR

Marco Tassi, Gunter Reekmans, Robert Carleer and Peter Adriaensens

1-Applied and Analytical Chemistry, Institute for Materials Research (IMO), Hasselt University, Agoralaan 1 - Building D, B-3590 Diepenbeek, Belgium

KEYWORDS: Hybrid materials, TiO_2 surface modification, structural quantification, ^{31}P solid state MAS NMR, phosphonic acid

ABSTRACT: For the first time, an absolute quantification of hybrid materials obtained from the reaction of phenylphosphonic acid (PPA) with TiO_2 nanoparticles under different reaction conditions is reported. Next to the amount of PPA involved in grafting to the TiO_2 nanoparticles, also the PPA included in titaniumphenylphosphonate crystallites is described quantitatively. The quantitative analysis is based on solid state ^{31}P MAS NMR and is further applied to evaluate the stability of the resulting hybrid materials towards hydrolysis and organic solvent exposure.

INTRODUCTION

In the past 30 years, the development of organic-inorganic hybrid materials attracted the attention of many scientists[1,2,3,4] since the combination of inorganic and organic properties revealed to be functional in many applications[5] such as coatings[6], gas storage[7], separation processes[8,9], catalysis[10] and optical device production[11]. In this framework, the scientific community focused its efforts on the development of synthesis pathways dedicated to form stable bonds between the organic and the inorganic species[12,13,14]. Surface grafting of inorganic substrates by incorporating organic monolayers revealed to be one of the most studied pathways for producing hybrid materials[14,15,16]. Many examples of such materials, composed of metal oxide surfaces modified by organic coupling molecules such as organosilanes or organophosphorous compounds are reported in literature[12,17,18,19,20]. Surface grafting of

metal oxide supports anchoring organosilanes (i.e. organoalkoxysilanes, organohalosilanes or organoaminosilanes) can only by formation of M-O-Si-R bonds (M = transition metal) [21,22]. However, a limited stability of such organic layers is observed, due to the vulnerability of M-O-Si-R bonds towards hydrolysis[23]. Also phosphonic acids have been used to introduce new properties at the surface of metal oxides via heterocondensation between the metal oxide hydroxyl groups and the P-OH groups of the phosphonic acid[14,24,25,26]. This reaction results in more stable M-O-P-R bonds[23]. A stable layer can be formed by the reaction of TiO_2 with phosphonic acid in monodentate or bidentate binding modes[19]. The phosphonic acid grafting methodology has been widely applied to TiO_2 nanoparticles[27] in order to produce multifunctional nanomaterials[28,29]. Guerrero et al. reported that the formation of a stable organic layer anchored at the TiO_2 surface can be obtained at room temperature[19,24]. It was also reported that the surface modification of TiO_2 at higher reaction temperatures also includes the formation of titaniumphosphonate resulting from the partial hydrolysis of the TiO_2 matrix[19,24]. ATR-FTIR, XRD, TEM and solid state ^{31}P, ^{13}C and ^{17}O NMR spectroscopy have been used to characterize the obtained titanium dioxide modified materials[19,24,30]. Solid state NMR in general is a strong technique for the structural characterization of materials[31,32,33]. In particular, ^{31}P solid state NMR revealed to be very important to differentiate between phosphonic acid involved in the surface modification of TiO_2 nanoparticles and the phosphonic acid involved in the formation of titaniumphosphonate since, depending on the reaction temperature, both species can be present together in the modified material[30]. From literature, it is clear that numerous papers deal with the qualitative characterization of phosphonic acid modified metal oxides[14,15,16,26]. However, very little attention has been paid to obtain quantitative data regarding the amount of PPA grafted to TiO_2 nanoparticles and the amount included in titaniumphosphonate. This paper introduces for the first time a method that allows a fully and absolute quantification of phosphonic acid modified TiO_2 nanoparticles, including the amount of PPA involved in TiO_2 surface grafting next to the amount involved in titaniumphenylphosphonate structures. Moreover, the stability in strong acid conditions and organic solvents was evaluated quantitatively. Last

but not least, the quantitative description of these modified TiO_2 materials by solid state ^{31}P-NMR might pave the way towards the design and production of property-tuned TiO_2 hybrid materials.

EXPERIMENTAL

Hydrophilic fumed P25 TiO_2 powder (Aeroxide), with a specific surface area of 50 m^2/g and an average primary particle size of 21 nm was used as substrate material. Phenylphosphonic acid ($PhPO_3H_2$, PPA, 98%, 158.09 MW) and octylphosphonic acid ($C_8PO_3H_{19}$, OPA, 97%, 194.21 MW) were obtained from Aldrich, analyzed for structure and purity by solid state magic angle spinning (MAS) ^{31}P-NMR and used without further purification. MilliQ water was used for all solutions.

TiO_2/PPA-20°C: 1 g (8.7 mmol) of TiO_2 was dispersed in 20 ml of a 0.1 M solution of PPA in water (316 mg/20 ml, 2 mmol). After stirring the reaction mixture for 24 h at 20°C, the solid was recovered by membrane filtration (VitraPOR Borosilicate 3.3) and washed with 200 ml water in order to remove remaining free PPA. Finally the material was dried at 120°C under vacuum for 24h.

TiO_2/PPA-45°C, TiO_2/PPA-90°C, TiO_2/PPA-120°C and TiO_2/PPA-150°C: 750 mg (6.5 mmol) of TiO_2 was dispersed in 15 ml of a 0.1 M solution of PPA in water (237 mg/15ml, 1.5 mmol). The reaction was carried out for 3 hours in a microwave reactor. The solid was recovered and dried as described above.

TiO_2/PPA-150°C-HCl-treated: 1g of TiO_2/PPA-150°C was dispersed in 15 ml HCl 1M at room temperature under stirring. After 12 hours the material was recovered by membrane filtration (VitraPOR Borosilicate 3.3) and washed with 800 ml of water. Finally the material was dried for 24 hours under vacuum.

TiO_2/OPA: 6 mg of OPA was dissolved in 1.5 ml acetone and dispersed with 114 mg of TiO_2. Subsequently, the acetone was evaporated at 60°C and the sample was analyzed by means of solid state ^{31}P MAS NMR**.**

TiO_2/PPA: 10 mg of PPA was dissolved in 2 ml acetone and dispersed with 100 mg of TiO_2. Subsequently, the acetone was evaporated at 60°C and the sample was analyzed by means of solid state ^{31}P MAS NMR.

Preparation of TiO_2/PPA-OPA samples for absolute quantification. In order to absolutely quantify the TiO_2/PPA samples, octylphosphonic acid was added as internal standard. The samples are coded TiO_2/PPA-x°C-OPA, with x°C the reaction temperature at which the TiO_2 was modified with PPA before. **TiO_2/PPA-20°C-OPA:** 6 mg of OPA was dissolved in 1.5 ml acetone and dispersed with 114 mg of TiO_2/PPA-20°C. Subsequently, the acetone was evaporated at 60°C, after which a known amount (in the order of 50 mg) was placed in a ceramic rotor for solid state MAS NMR analysis. The exact amount of material in the rotor was obtained from the weight difference between an empty and a filled rotor. **TiO_2/PPA-45°C-OPA** was prepared in the same way and 48 mg was put in the rotor for SS-NMR. **TiO_2/PPA-90°C-OPA:** 10 mg of OPA was dissolved in 1.5 ml of acetone and dispersed with 110 mg of TiO_2/PPA-90°C. Subsequently, the acetone was dried for 5 minutes at 60°C and 45 mg was used for SS-NMR. The samples **TiO_2/PPA-120°C-OPA, TiO_2/PPA-150°C-OPA, TiO_2/PPA-150°C-HCl-treated-OPA and TiO_2/PPA-150°C-post-SPE-OPA** were prepared in the same way as described for TiO_2/PPA-90°C-OPA.

Solid phase extraction (SPE) with TiO_2/PPA-150°C as stationary phase: 1.8 g of TiO_2/PPA-150°C material was packed in a solid phase extraction column and solid phase extraction was carried out following the CLWE procedure[34]. Conditioning of the material was carried out with 2 ml of water followed by loading a mixture composed of 1 ml methanol and 1 ml toluene. After recovery of the flow-

through, the solid phase was washed with 2 ml of water, followed by a final elution with 4 ml of cyclohexane. All operations were accomplished in a glass box (see Figure **S1**) under vacuum at a fixed pressure of 15 psi. After SPE, the stationary phase TiO_2/PPA-150°C material was recovered and washed several times with acetone and water, followed by drying at 120°C under vacuum for 24h. Regarding the eluted fractions, all were analyzed by liquid state ^1H NMR spectroscopy. ^1H liquid state NMR spectra were recorded at room temperature on a Varian Inova 300 spectrometer in a 5mm four-nucleus PFG probe. The chemical shift (δ) scale in ppm was calibrated relative to TMS (0 ppm). Other NMR parameters were: a 90° pulse of 4.0 μs, a spectral width of 5 kHz, an acquisition time of 4 s, a preparation delay of 12 s and 16 accumulations. A line-broadening factor of 0.2 Hz was applied before Fourier transformation to the frequency domain.

Solid state ^{31}P MAS NMR spectra were acquired at ambient temperature on an Agilent VNMRS DirectDrive 400MHz spectrometer (9.4 T wide bore magnet) equipped with a T3HX 3.2 mm probe dedicated for small sample volumes and high decoupling powers. Magic angle spinning (MAS) was performed at 10 kHz using ceramic zirconia rotors of 3.2 mm in diameter (22 μl rotors). The phosphorus chemical shift scale was calibrated to orthophosphoric acid (H_3PO_4) at 0 ppm. Other acquisition parameters used were: a spectral width of 50 kHz, a 90° pulse length of 3.6 μs, an acquisition time of 20 ms and 200-3000 accumulations. High power proton dipolar decoupling was set to 100 kHz during the acquisition time. Since the longest spin-lattice relaxation time (T1) registered was 250 s (for PPA physically adsorbed at the TiO_2 surface), a recycle delay of 1250 s was used in order to satisfy the condition to obtain fully quantitative results, i.e. using a recycle delay of 5x the longest T1 decay time. **For completeness, the T1 values measured for TiO_2/PPA prepared at 20°C, 45°C, 90°C, 120°C and 150°C are reported in Table 1**. The T1 decay time of TiO_2/OPA was 106 s.

Table 1: T1 values of the TiO_2/PPA materials.

Sample	T1 (s) of surface grafted PPA (23-2 ppm region)	T1 (s) of PPA in titaniumphosphonate (-4 ppm signal)
TiO_2/PPA-20°C	11	/
TiO_2/PPA-45°C	13	*ND
TiO_2/PPA-90°C	9	54
TiO_2/PPA-120°C	11	114
TiO_2/PPA-150°C	11	226

*ND: not determined as the signal is too small.

RESULTS AND DISCUSSION

Evaluation of OPA as internal standard for quantification. After reacting TiO_2 nanoparticles with phenylphosphonic acid (PPA) at different reaction temperatures, the PPA on the TiO_2 was characterized and quantified using solid state ^{31}P MAS NMR. For the quantification, octylphosphonic acid (OPA) was used as an internal standard. Hereto, OPA was mixed with the respective TiO_2/PPA-x°C powder in acetone (with x°C the reaction temperature at which the TiO_2 was modified with PPA), resulting in the final TiO_2/PPA-x°C-OPA powders after drying. Figure 1a shows the ^{31}P MAS spectrum of a dried TiO_2/OPA dispersion to demonstrate that the OPA signals do not interfere with the signals of free PPA at 21 ppm[30] (figure not shown) and the signal of a dried TiO_2/PPA dispersion (Figure 1b) which also shows a signal at 21 ppm. For all TiO_2/PPA species, the most downfield ^{31}P chemical shift is situated at 21 ppm, and so more upfield as compared to the OPA signals[30]. Remark that the signals of the dried TiO_2/OPA dispersion cover a region between 42 and 23 ppm due to the formation of covalent P-O-Ti bonds between OPA and TiO_2 in the dispersion. This is in agreement with literature, assigning the 42-23 ppm region to signals of OPA bonded to TiO_2[14].

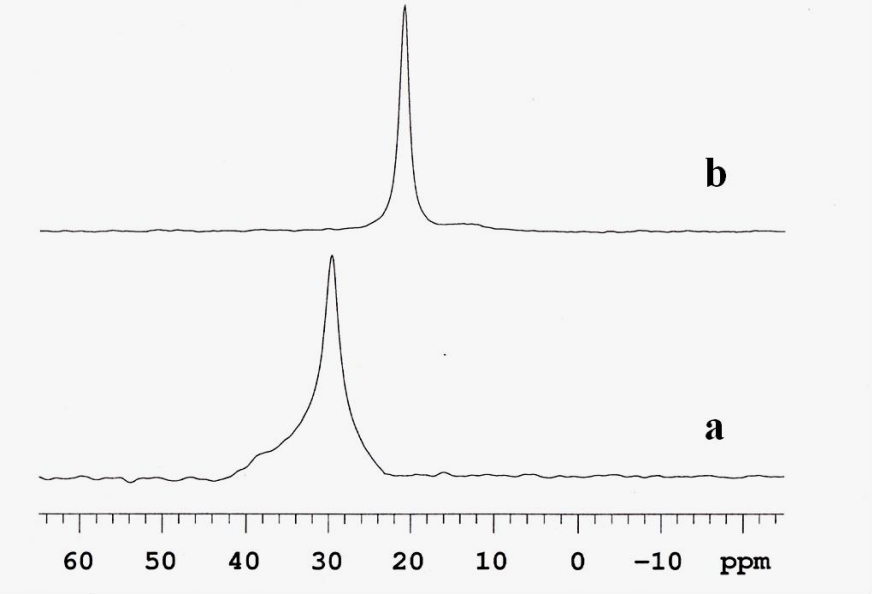

Figure 1: Solid state ^{31}P MAS NMR spectrum of a (a) dried dispersion of TiO_2/OPA and (b) dried dispersion of TiO_2/PPA.

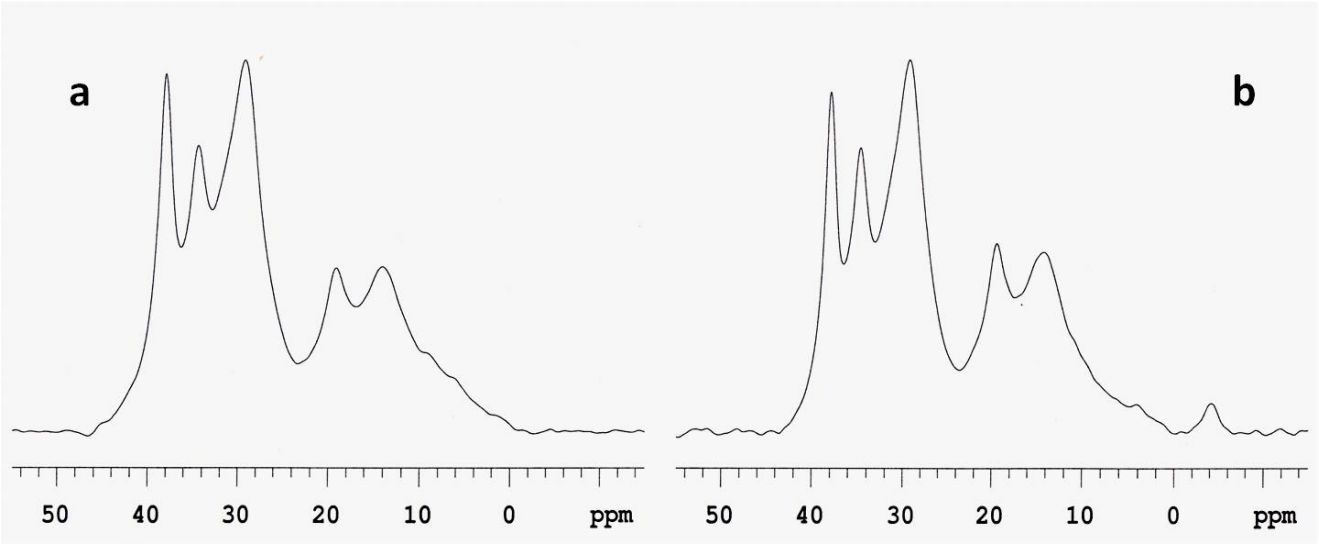

Figure 2: Solid state ^{31}P MAS NMR spectrum of (a) TiO_2/PPA-20°C-OPA and (b) TiO_2/PPA-45°C-OPA.

Figures 2-4 show ^{31}P MAS NMR spectra of different TiO_2/PPA-x°C-OPA materials. Figure 2 illustrates the ^{31}P MAS spectra of TiO_2/PPA-20°C-OPA (Figure **2a**) and TiO_2/PPA-45°C-OPA (Figure **2b**). Both spectra display three signals around 38, 34 and 28 ppm arising from OPA (42 ppm to 23 ppm region). Whereas the resonance at 38 ppm arises from OPA physically adsorbed at the TiO_2 surface, the

resonances at 34 and 29 ppm arise from OPA which is covalently bonded to the metal oxide via P-O-Ti bonds[14]. The presence of covalently bonded OPA at the TiO_2 surface indicates that there are still Ti-OH groups available after the reaction of PPA with TiO_2 at these temperatures. The PPA region (23-2 ppm) of TiO_2/PPA-20°C-OPA and TiO_2/PPA-45°C-OPA shows two bands at around 19 ppm and 14 ppm, arising from PPA grafted at the surface of the TiO_2 nanoparticles. The ^{31}P MAS spectrum of TiO_2/PPA-45°C-OPA shows a weak signal at -4 ppm in addition, indicating the presence of a minor amount of titaniumphenylphosphonate[26,35].

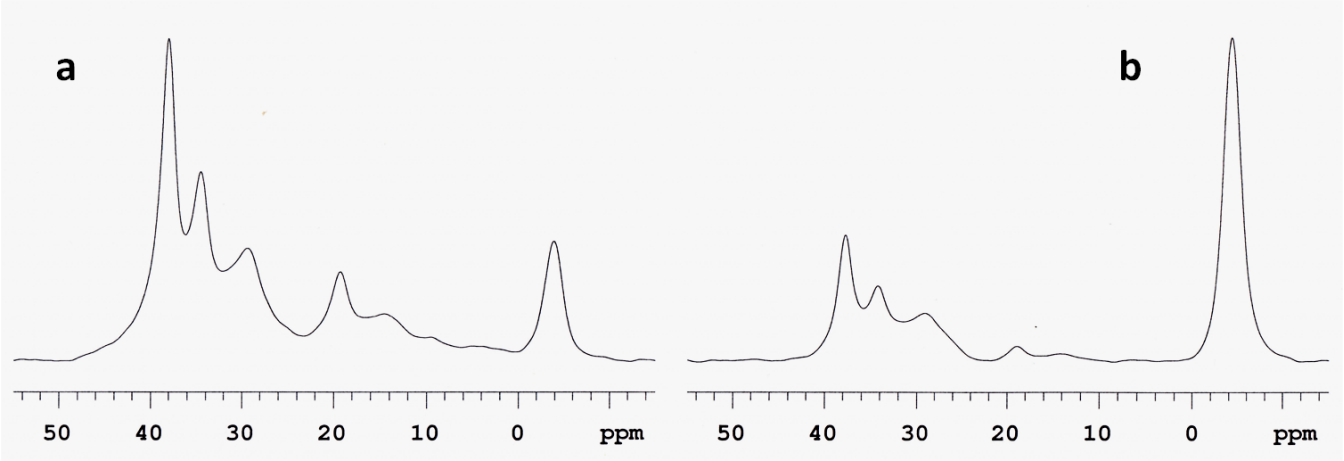

Figure 3: Solid state ^{31}P MAS NMR spectrum of (a) TiO_2/PPA-90°C-OPA and (b) TiO_2/PPA-120°C-OPA.

Figure 3 shows the ^{31}P MAS NMR spectra of TiO_2/PPA-90°C-OPA (Figure **3a**) and TiO_2/PPA-120°C-OPA (Figure **3b**). Remark that a somewhat larger amount of OPA had to be used since the amount of titaniumphenylphosphonate formed (signal at -4 ppm) starts to increase strongly as a function of the reaction temperature. This explains the relative change in the intensities of the three OPA signals in the region between 42 ppm and 23 ppm. In particular, the most significant difference is related to the increased intensity of the 38 ppm signal of OPA physically adsorbed at the TiO_2 surface. This can easily be explained by a larger amount of OPA standard that is physically adsorbed at the TiO_2 surface. The spectrum of TiO_2/PPA-90°C-OPA (Figure **3a**) further presents the 19 and 14 ppm signals from PPA grafted at the TiO_2 nanoparticles, but compared to the spectra of TiO_2/PPA-20°C-OPA and TiO_2/PPA-45°C-OPA (Figure 2), the intensity ratio of the 19 ppm/14 ppm signals is increased. This results from a

changing distribution of the different PPA-TiO_2 binding modes. Furthermore, the intensity of the -4 ppm resonance, assigned to titaniumphenylphosphonate, is increased noticeably. The ^{31}P MAS spectrum of TiO_2/PPA-120°C-OPA (Figure **3b)** shows a severe decrease of the 19 and 14 ppm signals, relatively to the strong increase of the -4 ppm signal. This indicates that the formation of titaniumphosphonate becomes predominant as compared to PPA grafting at the TiO_2 nanoparticles.

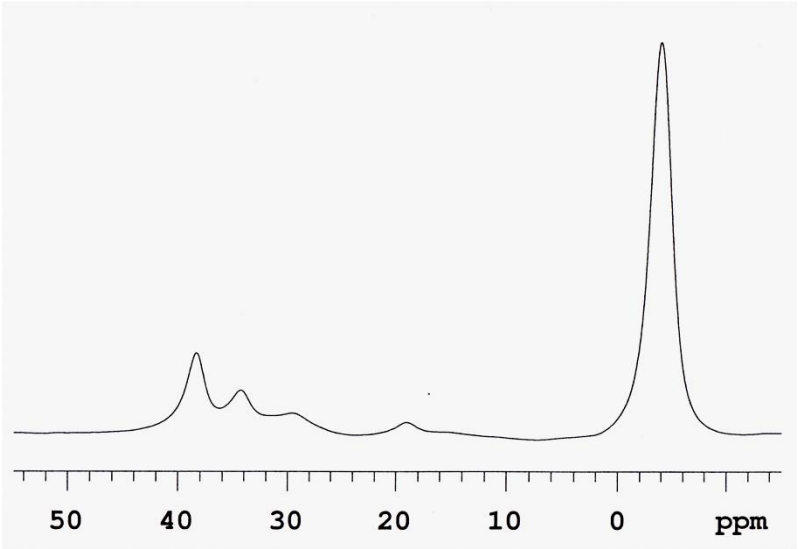

Figure 4: Solid state ^{31}P MAS NMR spectrum of TiO_2/PPA-150°C-OPA.

This trend is even more enhanced for TiO_2/PPA-150°C-OPA as shown in the ^{31}P MAS NMR spectrum (Figure 4). The spectrum is clearly dominated by the signal that represents titaniumphenylphosphonate at -4 ppm. Relatively to the titaniumphenylphosphonate signal, the signals around 19 and 14 ppm, characteristic for PPA grafted at the TiO_2 nanoparticles, become hardly visible.

Table 2: Quantification of PPA grafted at the TiO_2 nanoparticles surface for TiO_2/PPA-20°C, TiO_2/PPA-45°C TiO_2/PPA-90°C, TiO_2/PPA-120°C and TiO_2/PPA-150°C.

Specimen	PPA grafted at the TiO_2 surface in mmol/g *	PPA grafted at the TiO_2 surface in mg/g
TiO_2/PPA-20°C	0.10	15.8
TiO_2/PPA-45°C	0.13	20.5
TiO_2/PPA-90°C	0.12	19.0

TiO_2/PPA-120°C	0.11	17.4
TiO_2/PPA-150°C	0.08	13.2

*: the error is in the order of 0.01 mmol/g

Quantification of the amount of PPA grafted at the TiO_2 nanoparticle surface (see supporting information for more details). By integrating the quantitative ^{31}P MAS spectra (**Table S4**), the amount of PPA grafted at the TiO_2 surface can be determined for all specimens obtained from the reaction of PPA with TiO_2 at 20°C, 45°C, 90°C, 120°C and 150°C. The results are reported in **Table 2** from which it can be observed that the amount of PPA grafted at the TiO_2 nanoparticle surface only shows limited variation, indicating that the reaction temperature only has a minor effect on the amount of surface grafting. It further indicates that the amount of surface grafting under the applied reaction conditions (0.1 M PPA in water as solvent) is rather limited. The authors presume that this limited amount originates from the use of an excess of PPA which, once it is physically adsorbed to the TiO_2 surface, reduces the accessibility of the Ti-OH groups.

Table 3: Quantification of PPA involved in the titaniumphenylphosphonate structure for TiO_2/PPA-20°C, TiO_2/PPA-45°C, TiO_2/PPA-90°C, TiO_2/PPA-120°C and TiO_2/PPA-150°C.

Specimen	PPA in titaniumphenylphosphonate in mmol/g	PPA in titaniumphenylphosphonate in mg/g
TiO_2/PPA-20°C	/	/
TiO_2/PPA-45°C	0.004	0.7
TiO_2/PPA-90°C	0.08	12.1
TiO_2/PPA-120°C	0.5	84.6
TiO_2/PPA-150°C	1.3	206.4

*: the error is in the order of 0.01 mmol/g

*Quantification of the amount of PPA involved in titaniumphenylphosphonate structure*s. The quantification results regarding PPA involved in the titaniumphenylphosphonate formation are reported in **Table 3**. While no titaniumphenylphosphonate is observed in TiO_2/PPA-20°C, an increasing amount

is noticed as a function of the reaction temperature. A 325 fold increase of the molar amount of titaniumphenylphosphonate is obtained by increasing the reaction temperature from 45°C to 150°C. The quantification of TiO_2/PPA-90°C shows that for a reaction temperature of 90°C, the molar amount of PPA grafted at the TiO_2 nanoparticles (**Table 2**) is almost equal to the amount of PPA involved in titaniumphenylphosphonate (**Table 3**), i.e. the difference is only 0.04 mmol/g. For TiO_2/PPA-150°C, the amount of PPA in titaniumphenylphosphonate is even sixteen times higher than the amount of PPA grafted at the TiO_2 nanoparticles.

In conclusion it can be stated that the amount of PPA grafted at the TiO_2 nanoparticle surfaces is almost independent on the synthesis reaction temperature and so it will not influence the ratio PPA-grafted/titaniumphenylphosphonate. Conversely, the formation of titaniumphenylphosphonate becomes predominant in case of enhanced temperatures (T > 100°C).

Quantification of TiO_2/PPA-150°C-HCl-treated. In order to investigate the stability of the P-O-Ti bonds towards acid hydrolysis, TiO_2/PPA-150°C was exposed to a 1M solution of concentrated hydrochloric acid for 12 hours (TiO_2/PPA-150°C-HCl-treated). The ^{31}P MAS NMR spectrum of TiO_2/PPA-150°C-HCl-treated in the presence of the OPA standard (TiO_2/PPA-150°C-HCl-treated-OPA) is shown in the supporting information (Fig **S2**). **Table 4** shows the quantitative results of a comparison with the untreated TiO_2/PPA-150°C.

Table 4: Quantification of PPA in TiO_2/PPA-150°C and TiO_2/PPA-150°C–HCl-treated.

Sample	PPA grafted at the TiO_2 nanoparticles surface mmol/g	PPA grafted at the TiO_2 nanoparticles surface mg/g	PPA in titaniumphenylphosphonate mmol/g	PPA in titaniumphenylphosphonate mg/g
TiO_2/PPA-150°C	0.0830	13.2	1.30	206
TiO_2/PPA-150°C-HCl-treated	0.0012	0.2	1.29	204

*: the error is in the order of 0.01 mmol/g

The quantification of TiO_2/PPA-150°C-HCl-treated revealed that the amount of PPA involved in the titaniumphenylphosphonate structure remains unaffected. Prolonged acid treatment did not initiate hydrolysis of the $Ti(C_6H_5PO_3)_2$ units[36]. In contrast, **Table 4** illustrates that the amount of PPA grafted at the TiO_2 nanoparticles dramatically decreases as a result of the corrosive treatment. In fact, the PPA grafted at the TiO_2 surfaces in TiO_2/PPA-150°C-HCl-treated decreased with 98.5% as compared to the untreated TiO_2/PPA-150°C material, revealing that the surface grafted PPA is not resisting extremely hydrolytic conditions. This large difference in stability of P-O-Ti bonds in titaniumphenylphosphonate versus in grafted PPA can be explained by the self-assembly of the $Ti(C_6H_5PO_3)_2$ units into crystal layers with hydrophobic character, shielding the P-O-Ti bonds from the acid catalyzed hydrolysis. Conversely, the PPA grafted at the TiO_2 surfaces is not shielded and enhanced hydrolysis of these P-O-Ti bonds takes place.

Quantification of post solvent exposed TiO_2/PPA-150°C, i.e. after use as stationary phase in SPE experiments (TiO_2/PPA-150°C-post-SPE). SPE experiments were carried out in order to evaluate the stability of TiO_2/PPA-150°C towards organic solvents exposure. The stability of this class of hybrid materials in organic solvents is crucial since many dedicated and chromatography-related applications require materials operating under such conditions[37]. In addition, this experiment was also performed in order to evaluate the intrinsic hydrophobicity of the TiO_2/PPA-150°C material by using it as stationary phase in the SPE column for the separation of toluene from a 1/1 mixture of methanol/toluene (**Figure S1**). The hydrophobicity of the TiO_2/PPA-150°C is related to the amount of toluene kept in the extraction column after the loading step. It was measured that TiO_2/PPA-150°C was able to separate 91% of the toluene present in the methanol/toluene mixture. This high separation efficiency can be explained by the strong hydrophobic and Van der waals interactions between toluene and the phenyl ring of PPA at the outside of the titaniumphenylphosphonate crystals[35] and at the nanoparticles surface. After the chromatography, the structural composition of the resulting material was evaluated by quantitative ^{31}P MAS NMR using the OPA standard. The spectrum of TiO_2/PPA-150°C-post-SPE-OPA

is shown in the supporting information (Fig **S3**). **Table 5** reveals the characteristics of TiO_2/PPA-150°C before and after SPE.

Table 5: Quantification of PPA in TiO_2/PPA-150°C and TiO_2/PPA-150°C-post SPE.

Sample	PPA grafted at the TiO_2 nanoparticles surface mmol/g	PPA grafted at the TiO_2 nanoparticles surface mg/g	PPA in titaniumphenylphosphonate mmol/g	PPA in titaniumphenylphosphonate mg/g
TiO_2/PPA-150°C	0.083	13.2	1.30	206
TiO_2/PPA-150°C-post SPE	0.050	7.9	1.28	202

*: the error is in the order of 0.01 mmol/g

Similar as for TiO_2/PPA-150°C-HCl-treated (**Table 4**), the amount of PPA in the titaniumphenylphosphonate did not change significantly by the SPE. This indicates a high stability of the titaniumphenylphosphonate structure towards the exposure to apolar solvents like toluene and cyclohexane. This in contrast to a loss of 43% of the PPA grafted at the TiO_2 nanoparticles. This points to a loss of PPA modified nanoparticles during the CLWE (conditioning-loading-washing-elution) procedure of the SPE experiment[34].

CONCLUSIONS

For the first time the absolute quantification of phosphonic acid (PPA) modified TiO_2 nanoparticles is reported, and this by means of ^{31}P MAS NMR and with using octylphosphonic acid as internal standard. By this method, it was further possible to quantify the PPA grafted at the TiO_2 surface separately from the titaniumphenylphosphonate originating from the dissolution of the amorphous part of the matrix at enhanced reaction temperatures. From measurements of hybrid materials obtained by reacting PPA with TiO_2 as a function of increasing reaction temperature, it can be established that the amount of PPA grafted at the TiO_2 nanoparticles surface is quasi independent on the reaction temperature. The amount of PPA involved in titaniumphenylphosphonate formation on the other hand is strongly dependent on the reaction temperature. At reaction temperatures above 100°C, titaniumphenylphosphonate is

predominantly formed. The proposed methodology also allows to evaluate the materials stability under acid, corrosive conditions. The ^{31}P MAS NMR spectra demonstrate that PPA grafted at the TiO_2 nanoparticles is strongly vulnerable to acid induced hydrolysis while the titaniumphenylphosphonate is extraordinary stable. Regarding solid phase extraction (SPE), it is observed that a part of the PPA modified nanoparticles is lost during the extraction of a 1/1 methanol/toluene mixture but that all of the titaniumphenylphosphonate is preserved. Thus, the quantification method allows scientists to fine-tune these TiO_2 hybrid materials and application engineers to evaluate the structure-properties relation and the influence of annealing stress hereon.

ASSOCIATED CONTENT

Supporting information file contains the figures: supporting information 1, supporting information 2, supporting information 3 and the paragraph "Quantitative evaluation of the solid state ^{31}P MAS NMR spectra"

AUTHOR INFORMATION

Corresponding Authors:

Email: marco.tassi@uhasselt.be , robert.carleer@uhasselt.be

Author contributions

The manuscript was written through the contributions of all authors. All authors have given approval to the final version of the manuscript.

Notes

The authors declare no competing financial interest.

ACKNOWLEDGMENT

This work is financially supported by the Fund for Scientific Research of Flanders (FWO-Vlaanderen) via the project G.O127.12N. We further acknowledge the financial support from the Interuniversity Attraction Poles Programme (P7/05) initiated by the Belgian Science Policy Office (BELSPO).

REFERENCES

(1) Judeinstein, P.; Sanchez, C. Hybrid Organic–inorganic Materials: A Land of Multidisciplinarity. *J. Mater. Chem.* **1996**, *6* (4), 511–525.

(2) Frank Hoffmann, M. C. Silica-Based Mesoporous Organic–Inorganic Hybrid Materials. *Angew. Chem. Int. Ed Engl.* **2006**, *45* (20), 3216–3251.

(3) Hagrman, null; Hagrman, null; Zubieta, null. Organic-Inorganic Hybrid Materials: From "Simple" Coordination Polymers to Organodiamine-Templated Molybdenum Oxides. *Angew. Chem. Int. Ed Engl.* **1999**, *38* (18), 2638–2684.

(4) Zhu, Y.-P.; Yuan, Z.-Y. History and Classification of Non-Siliceous Hybrid Materials. In *Mesoporous Organic-Inorganic Non-Siliceous Hybrid Materials*; SpringerBriefs in Molecular Science; Springer Berlin Heidelberg, 2015; pp 7–23.

(5) Behzad Rezaei, H. M. Applications of Titanium Dioxide Nanoparticles. **2009**.

(6) Diebold, U. The Surface Science of Titanium Dioxide. *Surf. Sci. Rep.* **2003**, *48* (5–8), 53–229.

(7) Farha, O. K.; Yazaydın, A. Ö.; Eryazici, I.; Malliakas, C. D.; Hauser, B. G.; Kanatzidis, M. G.; Nguyen, S. T.; Snurr, R. Q.; Hupp, J. T. De Novo Synthesis of a Metal-Organic Framework Material Featuring Ultrahigh Surface Area and Gas Storage Capacities. *Nat. Chem.* **2010**, *2* (11), 944–948.

(8) Randon, J.; Paterson, R. Preliminary Studies on the Potential for Gas Separation by Mesoporous Ceramic Oxide Membranes Surface Modified by Alkyl Phosphonic Acids. *J. Membr. Sci.* **1997**, *134* (2), 219–223.

(9) Randon, J.; Blanc, P.; Paterson, R. Modification of Ceramic Membrane Surfaces Using Phosphoric Acid and Alkyl Phosphonic Acids and Its Effects on Ultrafiltration of BSA Protein. *J. Membr. Sci.* **1995**, *98* (1–2), 119–129.

(10) Tao Miao, L. W. Immobilization of Copper in Organic—Inorganic Hybrid Materials: A Highly Efficient and Reusable Catalyst for the Ullmann Diaryl Etherification. *Cheminform* **2007**, *38* (15).

(11) R. Houbertz, G. D. Inorganic-Organic Hybrid Materials for Application in Optical Devices. Thin Solid Films 442, 194-200. *Thin Solid Films* **2003**, *442* (1), 194–200.

(12) Castricum, H. L.; Sah, A.; Mittelmeijer-Hazeleger, M. C.; ten Elshof, J. E. Hydrophobisation of Mesoporous Γ-Al2O3 with Organochlorosilanes—efficiency and Structure. *Microporous Mesoporous Mater.* **2005**, *83* (1–3), 1–9.

(13) Sperling, R. A.; Parak, W. J. Surface Modification, Functionalization and Bioconjugation of Colloidal Inorganic Nanoparticles. *Philos. Trans. R. Soc. Lond. Math. Phys. Eng. Sci.* **2010**, *368* (1915), 1333–1383.

(14) Gao, W.; Dickinson, L.; Grozinger, C.; Morin, F. G.; Reven, L. Self-Assembled Monolayers of Alkylphosphonic Acids on Metal Oxides. *Langmuir* **1996**, *12* (26), 6429–6435.

(15) Mutin, P. H.; Guerrero, G.; Vioux, A. Organic–inorganic Hybrid Materials Based on Organophosphorus Coupling Molecules: From Metal Phosphonates to Surface Modification of Oxides. *Comptes Rendus Chim.* **2003**, *6* (8–10), 1153–1164.

(16) Pramanik, M.; Patra, A. K.; Bhaumik, A. Self-Assembled Titanium Phosphonate Nanomaterial Having a Mesoscopic Void Space and Its Optoelectronic Application. *Dalton Trans.* **2013**, *42* (14), 5140–5149.

(17) Carrado, K. A.; Xu, L.; Csencsits, R.; Muntean, J. V. Use of Organo- and Alkoxysilanes in the Synthesis of Grafted and Pristine Clays. *Chem. Mater.* **2001**, *13* (10), 3766–3773.

(18) Nilsing, M.; Lunell, S.; Persson, P.; Ojamäe, L. Phosphonic Acid Adsorption at the TiO2 Anatase (1 0 1) Surface Investigated by Periodic Hybrid HF-DFT Computations. *Surf. Sci.* **2005**, *582* (1–3), 49–60.

(19) Guerrero, G.; Alauzun, J. G.; Granier, M.; Laurencin, D.; Mutin, P. H. Phosphonate Coupling Molecules for the Control of Surface/interface Properties and the Synthesis of Nanomaterials. *Dalton Trans.* **2013**, *42* (35), 12569–12585.

(20) Queffélec, C.; Petit, M.; Janvier, P.; Knight, D. A.; Bujoli, B. Surface Modification Using Phosphonic Acids and Esters. *Chem. Rev.* **2012**, *112* (7), 3777–3807.

(21) Rurack, K.; Martinez-Manez, R. *The Supramolecular Chemistry of Organic-Inorganic Hybrid Materials*; John Wiley & Sons, 2010.

(22) Helmy, R.; Fadeev, A. Y. Self-Assembled Monolayers Supported on TiO2: Comparison of C18H37SiX3 (X= H, Cl, OCH3), C18H37Si (CH3) 2Cl, and C18H37PO (OH) 2. *Langmuir* **2002**, *18* (23), 8924–8928.

(23) Marcinko, S.; Fadeev, A. Y. Hydrolytic Stability of Organic Monolayers Supported on TiO2 and ZrO2. *Langmuir* **2004**, *20* (6), 2270–2273.

(24) Guerrero, G.; Mutin, P. H.; Vioux, A. Anchoring of Phosphonate and Phosphinate Coupling Molecules on Titania Particles. *Chem. Mater.* **2001**, *13* (11), 4367–4373.

(25) Gervais, C.; Profeta, M.; Lafond, V.; Bonhomme, C.; Azaïs, T.; Mutin, H.; Pickard, C. J.; Mauri, F.; Babonneau, F. Combined Ab Initio Computational and Experimental Multinuclear Solid-State Magnetic Resonance Study of Phenylphosphonic Acid. *Magn. Reson. Chem.* **2004**, *42* (5), 445–452.

(26) Mutin, P. H.; Guerrero, G.; Vioux, A. Hybrid Materials from Organophosphorus Coupling Molecules. *J. Mater. Chem.* **2005**, *15* (35-36), 3761–3768.

(27) Chen, X.; Mao, S. S. Titanium Dioxide Nanomaterials: Synthesis, Properties, Modifications, and Applications. *Chem. Rev.* **2007**, *107* (7), 2891–2959.

(28) Neouze, M.-A.; Schubert, U. Surface Modification and Functionalization of Metal and Metal Oxide Nanoparticles by Organic Ligands. *Monatshefte Für Chem. - Chem. Mon.* **2008**, *139* (3), 183–195.

(29) Kango, S.; Kalia, S.; Celli, A.; Njuguna, J.; Habibi, Y.; Kumar, R. Surface Modification of Inorganic Nanoparticles for Development of Organic–inorganic nanocomposites—A Review. *Prog. Polym. Sci.* **2013**, *38* (8), 1232–1261.

(30) Brodard-Severac, F.; Guerrero, G.; Maquet, J.; Florian, P.; Gervais, C.; Mutin, P. H. High-Field 17O MAS NMR Investigation of Phosphonic Acid Monolayers on Titania. *Chem. Mater.* **2008**, *20* (16), 5191–5196.

(31) Tassi, M.; Bartollini, E.; Adriaensens, P.; Bianchi, L.; Barkakaty, B.; Carleer, R.; Chen, J.; Hensley, D. K.; Marrocchi, A.; Vaccaro, L. Synthesis, Characterization and Catalytic Activity of Novel Large Network Polystyrene-Immobilized Organic Bases. *RSC Adv.* **2015**, *5* (130), 107200–107208.

(32) Mens, R.; Bertho, S.; Chambon, S.; D'Haen, J.; Lutsen, L.; Manca, J.; Gelan, J.; Vanderzande, D.; Adriaensens, P. Solid-State NMR as a Tool to Describe and Quantify the Morphology of Photoactive Layers Used in Plastic Solar Cells. *J. Polym. Sci. Part Polym. Chem.* **2011**, *49* (7), 1699–1707.

(33) Adriaensens, P.; Storme, L.; Carleer, R.; Gelan, J.; Du Prez, F. E. Comparative Morphological Study of Poly(dioxolane)/Poly(methyl Methacrylate) Segmented Networks and Blends by 13C Solid-State NMR and Thermal Analysis. *Macromolecules* **2002**, *35* (10), 3965–3970.

(34) Gañán, J.; Pérez-Quintanilla, D.; Morante-Zarcero, S.; Sierra, I. Comparison of Different Mesoporous Silicas for off-Line Solid Phase Extraction of 17β-Estradiol from Waters and Its Determination by HPLC-DAD. *J. Hazard. Mater.* **2013**, *260*, 609–617.

(35) Clearfield, A.; Demadis, K. *Metal Phosphonate Chemistry: From Synthesis to Applications*; Royal Society of Chemistry, 2011.

(36) Alberti, G.; Casciola, M.; Costantino, U.; Vivani, R. Layered and Pillared metal(IV) Phosphates and Phosphonates. *Adv. Mater.* **1996**, *8* (4), 291–303.

(37) Liu, G.; Wei, W.; Jin, W.; Xu, N. Polymer/Ceramic Composite Membranes and Their Application in Pervaporation Process. *Chin. J. Chem. Eng.* **2012**, *20* (1), 62–70.